SWIMMING, PUMPING AND GLIDING AT LOW REYNOLDS NUMBER

Research Thesis

Submitted in partial fulfillment of the requirements for the degree of
Master of Science in Physics

Oren Raz

Submitted to the Senate of the Technion - Israel Institute of Technology
Hodesh 5768 HAIFA December 2007

This research thesis was done under the supervision of Associate Prof. Joseph Avron in the Faculty of Physics, and Prof. Alexander Leshansky in the Faculty of Chemical Engineering.

I would like to thank Dr. Oded kenneth for his contributions.

I would like to thank my wife Michal for her support.

The generous financial support of
The Technion
is gratefully acknowledged.

Contents

List of Figures

Abstract

This research is about micro-swimmers, micro-pumps and the relations between them. First, I study what swimming at low Reynolds number is, through few simple examples: the first one is the famous Purcell's three linked swimmer, made of three slender rods, which can control the angles between the rods. This example demonstrate the non-trivial behavior of even a very simple swimmer at low Reynolds number, and I use the Wilczek-Shapere formalism [30] to give a partial analysis for this swimmer (problems like optimal strokes are not considered). Since this swimmer is very complicated to analyzed, I introduce some modifications (symmetrization) on this swimmer, which makes it much simpler to analyzed. On this modified Pursell's swimmer I can carry on many calculations which are too complicated for the Purcell's three linked swimmer, like fastest stroke or most efficient stroke. I also introduce other modification that can explain how, in some cases, swimming can be better in more viscose fluid.

After understanding, through the examples, what swimming at low Reynolds is, I connect swimming to pumping an gliding, through the linearity of Stokes equation and the Lorenz reciprocity. It turns out that the relations between a swimmer, a glider and the pump one gets by anchoring the swimmer are simple, and can shed light on both swimmer and pumps property. I also solve some optimization problems, like what will be the optimal pitch for a helix as a pump ad as a swimmer and where to anchor a linear swimmer in order to get the best pump. I end up by giving examples for a swimmer that will not pump and a pump that will not swim.

List of Symbols

symbol	Meaning
$\mathbf{v}$	velocity field
$\mathbf{f}$	external force (per mass unit)
$\tilde{p}$	pressure
p	modified pressure
ρ	mass density
μ	dynamic viscosity
Φ	external potential
`U`	characteristic velocity
L	characteristic length
`Re`	Reynolds number
Σ	fluid volume
γ	a stroke
V	linear velocity
ω	angular velocity
$\mathbf{V}$	(V, ω) - 6 dimensional vector
π_{ij}	stress tensor
F	force
N	torque
$\mathbf{F}$	(F, N) - 6 dimensional vector
r	position
dS_j	surface element
θ_i, ϕ	angles in swimmers
x, y	position of a point in a swimmer

symbol	**Meaning**
l_i	arm length in a swimmer
η	arms ratio in Purcell's swimmer
$\mathbf{t}$	tangent unit vector
κ	aspect ratio of a slender body
$A; \mathcal{A}; \tilde{\mathcal{A}}$	gauge field
$F; \mathcal{F}; \tilde{\mathcal{F}}$	strength field
$\mathcal{R}$	rotation matrix
$S(\gamma)$	surface bounded by γ
ϵ	small parameter
ΔX	change in swimmers place after full stroke
E	energy dissipation in full stroke
$g_{a,b}$	the dissipation metric on shape space
P	Power
ε	swimmers efficiency
τ	stroke time
q	Lagrange multiplier
S_q	action
M	grand resistance matrix
K	resistance matrix (between F and V)
C	coupling matrix (between F and ω)
Ω	rotation resistance matrix (between N and ω)
R	antisymmetric matrix associated with r
H_{ij}	Oseen tesor
a	sphere radius
q	arm length
Δq	amplitude of changes in arm length

1 Introduction

1.1 Motivation

The last few decades showed a growing interest in swimming at the micro and nano scales, motivated by both biological and engineering problems: in biology, questions about microorganisms locomotion inspired research on flagellar propulsions [13, 20, 29] and some other propulsion techniques as well [11, 27, 15], while the engineering effort to build artificial micro-swimmers [25, 16, 21] has led to questions about other aspects of swimming at low Reynolds.

The following work has two parts: the first one is about some specific problems in swimming at low Reynolds number (the Purcell's three linked swimmer and some modifications of this swimmer), and the second one is about general correlations between swimmers, pumps and dragged bodies (gliders) at low Reynolds number. Both of these problems were inspired by experimental questions: the Purcell's three linked swimmer is a first order approximation for a swimmer built by Gabor Kosa and Moshe Shoham [16] in the Mechanical Engineering faculty at the Technion, and the swimmer-pump relations where motivated by both the need of microscopic pumps [14] for "Lab on a Chip devices" and the experimental comfort of measuring bolted swimmers rather than free ones [4, 32].

1.2 Low Reynolds numbers hydrodynamics - Stokes equation

As has been stressed nicely in Purcell's canonical paper "Life at Low Reynolds number" [23], motion at the micro scale is different from our everyday experiences. Here I shall give a short derivation for the stokes equation which governs the motion of micro swimmers, pumps and gliders.

The fundamental equations governing motion of bodies in an incompressible fluid are Naviar-Stokes equations (together with the incompressibility equation) [17]:

$$\rho\left(\frac{\partial \mathbf{v}}{\partial t}+\left(\mathbf{v}\cdot\nabla\right)\mathbf{v}\right)=\rho\mathbf{f}-\nabla\tilde{p}+\mu\triangle\mathbf{v}\quad;\quad\nabla\cdot\mathbf{v}=0 \tag{1.1}$$

where $\mathbf{v}$ is the velocity field, ρ is the mass density, $\mathbf{f}$ is external force per mass unit (eg. gravity), $\tilde{p}$ is the pressure field and μ is the viscosity of the fluid. In the cases of constant ρ and when $\mathbf{f}$ is caused by some potential (that is $\mathbf{f}=-\nabla\Phi$ for some potential Φ), we can use the *modified pressure* to unified the pressure and volume force in Eq. (1.1): $p=\tilde{p}+\rho\Phi$,

and $\nabla p = \nabla \tilde{p} - \rho \mathbf{f}$. Under these assumptions Eq. (1.1) becomes

$$-\rho \left((\mathbf{v} \cdot \nabla) \mathbf{v} + \frac{\partial \mathbf{v}}{\partial t} \right) + \mu \triangle \mathbf{v} = \nabla p$$

The firs term in the left hand side of this equation is called the inertia term, and the second one is called the viscosity term. If the characteristic length of the problem at hand is L, the characteristic velocity is $\mathtt{U}$ and the time scale for the changes in $\mathbf{v}$ is comparable with $\frac{L}{\mathtt{U}}$, we can approximate the order of the Inertia and viscosity terms as: $\frac{\rho \mathtt{U}^2}{L}$ and $\frac{\mu \mathtt{U}}{L^2}$, respectively. The ratio between the inertial and the viscosity terms is called the Reynolds number, and is given by:

$$\mathtt{Re} = \frac{\rho \mathtt{U} L}{\mu}$$

In cases $\mathtt{Re} \ll 1$, the inertial term can be neglected from the equation, and the remain equations will be

$$\nabla p = \mu \triangle \mathbf{v} \quad ; \quad \nabla \cdot \mathbf{v} = 0 \tag{1.2}$$

The first one is known as Stokes equation, and the second one is the incompressibility equation. The physical characters of systems with a very low Reynolds number is that inertia is completely negligible: the movement of a body depends only on the instantaneous forces acting on it, and not on the velocity it had in the past – there is no "memory" in the system. This also means that at low Reynolds number a body is consider to be in a constant (angular) velocity, although the constant might changes with time: the acceleration time is negligible, so that at any moment the (angular) velocity is considered as a constant, with zero (angular) acceleration. This implies that the sum of all forces (torques) on a body is always zero. In the case of dragged/anchored body, the total force (torque) the fluid applies on a body is equal in magnitude but opposite in sign to the dragging/anchoring force (torque). In the case of a free body (like a swimmer), where all the forces (toques) are inner ones and thus summed to zero, the friction forces (torques) applied by the fluid on the body must also summed to be zero.

1.3 Lorenz Reciprocity

The exact solutions to Eq. (1.2) in three dimensions are known for only small number of geometries [12]: ellipsoids. Good approximations are known only for cases of many spheres [12] using Oseen tensor, and slender filaments [5], using "Slender body approximation". This will limit the types of swimmers we can analyze. Even in this limit class of geometries, the general solutions are usually hard.

However, not always exact solutions are necessary: in some cases, we can use general properties of the solutions of Eq. (1.2) without solving them explicitly. One such important property is the Lorenz reciprocity: Lorentz reciprocity says that if (v_j, π_{jk}) and (v'_j, π'_{jk}) are the velocity and stress fields for two solutions of the Stokes equations in the domain Σ then [12]:

$$\int_{\partial\Sigma} v'_i \, \pi_{ij} \, dS_j = \int_{\partial\Sigma} v_i \, \pi'_{ij} \, dS_j \tag{1.3}$$

This relation is a direct consequence of the Stokes equation. In order to prove it, we will firs write the stress field explicitly:

$$\pi_{ij} = \mu \left(\partial_i v_j + \partial_j v_i \right) - \delta_{ij} p$$

Using the stress tensor, Eq. (1.2) can be written as:

$$\partial_j \pi_{ij} = 0 \quad ; \quad \partial_j v_j = 0$$

Starting from $\int_{\partial\Sigma} v'_i \, \pi_{ij} \, dS_j$ and using Stokes theorem:

$$\int_{\partial\Sigma} v'_i \, \pi_{ij} \, dS_j = \int_{\Sigma} (\partial_j v'_i \, \pi_{ij} \; + v'_i \, \partial_j \pi_{ij} \,) dv$$

The last term in the right hand side of this equation is zero due to Stokes equation. Using the symmetry of the stress tensor and the incompressibility, we can rewrite the left hand side as:

$$\int_{\partial\Sigma} v'_i \, \pi_{ij} \, dS_j = 0.5 \int_{\Sigma} (\partial_j v'_i + \partial_i v'_j) \mu (\partial_j v_i + \partial_i v_j) dv$$

Since the above expression is symmetric in v and v', Eq. (3.20) follows.

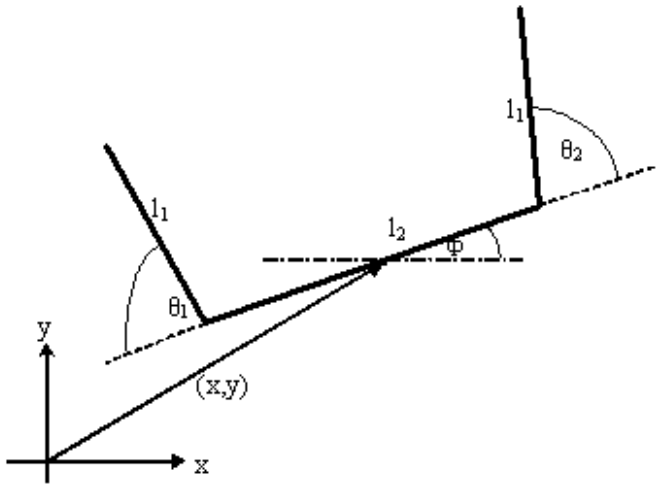

Figure 1: Purcell's three linked rods

2 Purcell's three linked swimmer, and it's symmetrizations

2.1 Introduction

Our aim in this part is to analyze, using Wilczek-Shapere formalism [30], the purcell's three-linked-rods swimmer [23], and to show the advantages and the intuition one can gain from this formalism. To fully appreciate the advantages of this formalism, we will introduce some generalizations of Purcell's three linked rods, where one can find analytical solutions to problems like "What is the most efficient stroke of the swimmer" or "what is the fastest stroke for the swimmer", and where the formalism can give simple explanations to some other problems, like the fact that in some cases [9] the swimming distance and efficiency can grow with the viscosity of the fluid .

2.2 Purcell's three linked swimmer

In his famous talk "Life at low Reynolds numbers" [23], M. E. Purcell introduced a simple swimmer built from three linked rods, as shown in Fig. (1). As an exercise for students, Purcell asked "what will determine the direction this swimmer will swim?". Although simple looking , this question was answered only about 15 years later by H. Stone et. al.

[3]. They have found that the direction of swimming depends, among other things, on the stroke's amplitude. Apparently, this simple looking swimmer is far from being simple to analyzed, and it's general stroke can only be analyzed numerically. Purcell's three linked rods had also been investigated for refine slender body approximation and general strokes by Hosoi et. al. [6].

In order to analyze this swimmer, we will first set up the notation: As in figure (1), we will note the angle between the middle link and the first arm as θ_1, and the angle between the middle link and the second arm as θ_2. The set (θ_1, θ_2) is called "the shape" of the swimmer, and is a point in the "shape space" of the Purcell's swimmer, $(\theta_1, \theta_2) \in [-\pi, \pi] \times [-\pi, \pi]$. A swimming stroke is then a closed, non self-intersecting continues path in the swimmer's shape space. We will take the lengths of the outer arms to be l_1, the middle arm to be l_2 and will mark $\eta = \frac{l_2}{l_1}$. η is fixed for a given swimmer, but one can ask questions about swimmers with different η.

Since we are interested in the locomotion of the swimmer due it's shape changes – we need some (arbitrary) reference frame to measure it. Let us fix an arbitrary reference frame in the plane of the swimmer, and measure the position of the swimmer as the position (x, y) of the middle point of the middle link (the choice of point in the body, together with the reference frame, serves as gauge fixing [30] in the problem). The angle between the middle link and the x axis is marked as ϕ. The complete information on the swimmer's position and shape (in the language of [30] and from here on - "Located shape") is the set $(x, y, \phi, \theta_1, \theta_2)$. Our problem is to determine the located shape of the swimmer, due to it's changes in shape space: to calculate the changes in x, y, ϕ (the response) due to the changes in θ_1, θ_2 (the controls).

In order to calculate the responses $dx, dy, d\phi$ as functions of the controls $d\theta_1, d\theta_2$, we can use the fact that all the forces due to shape changes are inner forces, and thus the total force on the swimmer is zero. Using Cox slender body theory [5] to first order,

$$dF(x) = k(\mathbf{t}(\mathbf{t} \cdot \mathbf{v}) - 2\mathbf{v})dx, \quad k = \frac{2\pi\mu}{\ln \kappa} \tag{2.4}$$

where $\mathbf{t}(x)$ is a unit tangent vector to the slender-body at x and $\mathbf{v}(x)$ the velocity of the point x of the body, one can calculate the velocities $\dot{x}, \dot{y}, \dot{\phi}$ of the swimmer from the located shape $(x, y, \phi, \theta_1, \theta_2)$ and the change in shape $(\dot{\theta_1}, \dot{\theta_2})$. The response-control equation is, due to the linearity of the force and torque equations, of the form:

$$\begin{pmatrix} dx \\ dy \\ d\phi \end{pmatrix} = dr^\alpha = \mathcal{A}_i^\alpha(x, y, \phi, \theta_1, \theta_2)d\theta_i = \mathcal{A} \begin{pmatrix} d\theta_1 \\ d\theta_2 \end{pmatrix} \tag{2.5}$$

where $\mathcal{A}$ is a 3×2 matrix, upper Greek letters are the response (row) indexes $(dx, dy, d\theta)$ and lower Roman letters are the controls (column) indexes $(d\theta_1, d\theta_2)$. It is clear that $\mathcal{A}_i^\alpha$ cannot be dependent on (x, y), due the translation symmetry of the system. The only way $\mathcal{A}_i^\alpha$ can be dependent on ϕ is

$$\mathcal{A}_i^\alpha\left(\phi,\theta_1,\theta_2\right)=\mathcal{R}^{\alpha\beta}(\phi)\tilde{A}_i^\beta\left(\theta_1,\theta_2\right);\quad \mathcal{R}^{\alpha\beta}\left(\phi\right)=\begin{pmatrix}\cos\phi & -\sin\phi & 0\\ \sin\phi & \cos\phi & 0\\ 0 & 0 & 1\end{pmatrix}$$

since the system has a rotation symmetry also. The total change in the swimmers position due a stroke γ is given by

$$\Delta r^\alpha=\oint\limits_\gamma \mathcal{A}_i^\alpha d\theta_i=\frac{1}{2}\int\limits_{S(\gamma)}\left(\frac{\partial\mathcal{A}_i^\alpha}{\partial\theta_j}-\frac{\partial\mathcal{A}_j^\alpha}{\partial\theta_i}\right)d\theta_i\wedge d\theta_j\equiv\frac{1}{2}\int\limits_{S(\gamma)}\mathcal{F}_{ij}^\alpha d\theta_i\wedge d\theta_j$$

where $S(\gamma)$ is the oriented surface bounded by γ. The orientation means that changing the stroke's direction is changing the orientation of the surface $(d\theta_i\wedge d\theta_j=-d\theta_j\wedge d\theta_i)$. We can now calculate $\mathcal{F}_{ij}^\alpha$:

$$\mathcal{F}_{ij}^\alpha=\partial_i\mathcal{A}_j^\alpha-\partial_j\mathcal{A}_i^\alpha=\mathcal{R}^{\alpha\beta}\left(\partial_i\tilde{\mathcal{A}}_j^\beta-\partial_j\tilde{\mathcal{A}}_i^\beta\right)+\left(\partial_i R^{\alpha\beta}\right)\tilde{\mathcal{A}}_j^\beta-\left(\partial_j\mathcal{R}^{\alpha\beta}\right)\tilde{\mathcal{A}}_i^\beta \tag{2.6}$$

It is easy to verify that

$$\partial_i\mathcal{R}^{\alpha\beta}=\varepsilon^{\beta\delta\phi}\mathcal{R}^{\alpha\delta}\tilde{\mathcal{A}}_i^\phi \tag{2.7}$$

where $\varepsilon^{\beta\delta\phi}$ is the antisymmetric tensor. Plugging Eq.(2.7) inside Eq.(2.6) (relabeling the indices β,δ), we get:

$$\mathcal{F}_{ij}^\alpha=\mathcal{R}^{\alpha\beta}\left(\partial_i\tilde{\mathcal{A}}_j^\beta-\partial_j\tilde{\mathcal{A}}_i^\beta+\varepsilon^{\delta\beta\phi}\left(\tilde{\mathcal{A}}_i^\phi\tilde{\mathcal{A}}_j^\delta-\tilde{\mathcal{A}}_j^\phi\tilde{\mathcal{A}}_i^\delta\right)\right)\equiv\mathcal{R}^{\alpha\beta}\tilde{\mathcal{F}}_{ij}^\beta$$

For small strokes $\Delta\theta=\epsilon$, we can approximate:

$$\Delta r^\alpha=\frac{1}{2}\int\limits_{S(\gamma)}\mathcal{R}^{\alpha\beta}(\phi)\tilde{\mathcal{F}}_{ij}^\beta d\theta_i\wedge d\theta_j\simeq\mathcal{R}^{\alpha\beta}(\phi)\frac{1}{2}\int\limits_{S(\gamma)}\tilde{\mathcal{F}}_{ij}^\beta d\theta_i\wedge d\theta_j+O(\epsilon^3) \tag{2.8}$$

This structure for $\tilde{\mathcal{A}}_i^\alpha$ and $\tilde{\mathcal{F}}_{ij}^\alpha$ is exactly the structure of a non-abelian gauge potential and field.

Pay attention for a few interesting consequences (we will use $\mathcal{F}^\alpha$ as a short name for $\mathcal{F}_{12}^\alpha$, etc'):

- There is no approximation in $\Delta\phi = \frac{1}{2}\int \tilde{\mathcal{F}}^{\phi}_{ij} d\theta_i d\theta_j$, so one can calculate $\Delta\phi$ for any stroke by surface integrating over $\tilde{\mathcal{F}}^{\phi}$. Since the total rotation of the swimmer does not depend on the point we choose to specify the swimmer position, $\tilde{\mathcal{F}}^{\phi}$ is gauge invariant. This function is too complicated to give it here. A plot of it is given in Fig. (2) for $\eta = 2$.

- For small strokes (or moderate strokes in which ϕ almost doesn't change), one can approximate the changes in the position x, y by integrating $\tilde{\mathcal{F}}^{x}$ and $\tilde{\mathcal{F}}^{y}$ respectively over the stroke aria, and use the rotating matrix. $\tilde{\mathcal{F}}^{x}$ and $\tilde{\mathcal{F}}^{y}$ are *not* gauge invariant, and depend on the way we decided to measure the swimmer's position. $\tilde{\mathcal{F}}^{x}$ and $\tilde{\mathcal{F}}^{y}$ are again too complicated to give them explicitly, and they are plotted in Fig. (3), for $\eta = 2$ and the position measured at the center of the middle link.

The Purcell's swimmer has two important symmetries, as discussed in [6, 3], which can be seen from the figures of $\tilde{\mathcal{F}}$ (Figs. 2,3): a reflection symmetry around the $\theta_1 = \theta_2$ axis, and a reflection symmetry around the $\theta_1 = -\theta_2$ axis. A reflection around the $\theta_1 = \theta_2$ axis is just a reflection of the swimmer around the central vertical of the middle link and a reflection around the $\theta_1 = \theta_2$ axis is just a rotation of the swimmer by π. Since reflecting a curve will change it's orientation, we can see that:

- The rotation of the swimmer will just change sign due reflecting around the central vertical, thus $\tilde{\mathcal{F}}^{\phi}$ must be *symmetric* around the $\theta_1 = \theta_2$ axis. The rotation will not be changed due to rotation of the swimmer, thus $\tilde{\mathcal{F}}^{\phi}$ must be *antisymmetric* around the $\theta_1 = -\theta_2$ axis. These symmetries can be seen in Fig. (2).

- Since we choose to describe the swimmer at a point that will not be changed in both reflection around the central vertical of the middle rod and rotating the swimmer by π, we can also see symmetries in $\tilde{\mathcal{F}}^{x}$ and $\tilde{\mathcal{F}}^{y}$: reflecting around the central vertical will change the sign of the velocity of the swimmer in the middle link direction (the x axis) and will not effect the velocity in the perpendicular direction, so $\tilde{\mathcal{F}}^{x}$ must be *symmetric* and $\tilde{\mathcal{F}}^{y}$ must be *antisymmetric* around $\theta_1 = \theta_2$. A π rotation will change the sign of the displacement in both x and y directions, so both $\tilde{\mathcal{F}}^{x}$ and $\tilde{\mathcal{F}}^{y}$ must be symmetric around $\theta_1 = -\theta_2$. These symmetries can be seen in Fig. (3). They are not gauge invariant, and will not be exist for generally chosen gauge.

- The plot of $\tilde{\mathcal{F}}^{x}$ in Fig. (3) can explain the fact that the swimmer swims in different directions for small and large rectangular strokes around $\theta_1 = \theta_2 = 0$, as discussed in [3]: from Fig. (3) it is clear that $\tilde{\mathcal{F}}^{x}$ changes it's sign. For small strokes the sign is

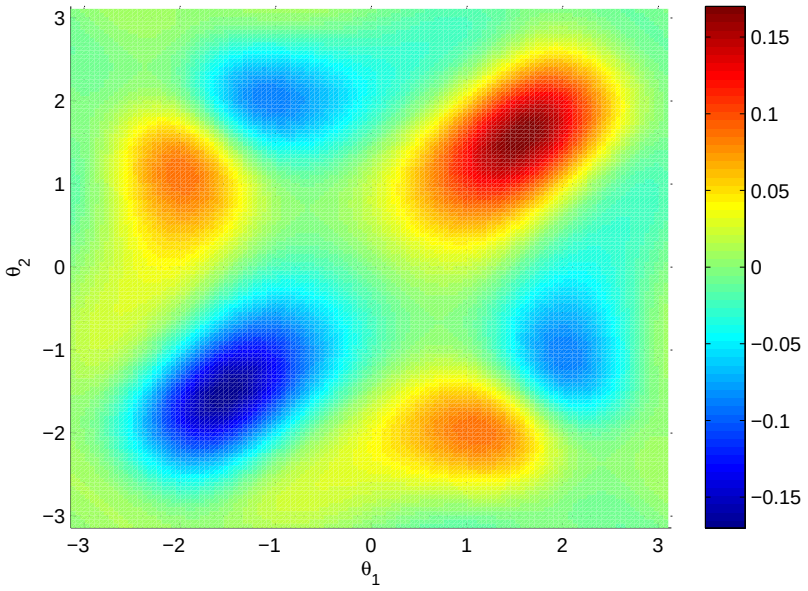

Figure 2: $\tilde{\mathcal{F}}^{\phi}(\theta_1, \theta_2)$ for Purcell's three linked swimmer (in radians)

negative. Since for rectangular strokes the change in ϕ is moderate (this can be seen from the small values of $\tilde{\mathcal{F}}^{\phi}$ and the symmetry of the problem), we can approximate the displacement in the x direction by integrating $\tilde{\mathcal{F}}^{x}$ even for moderate strokes. Since the sign is changed, the direction of the swimming will also be changed.

2.3 The symmetric purcell's swimmer

As discussed in the previous chapter, the "Purcell's three linked rod", which was invented as "The simplest animal that can swim that way..." [23], is not simple at all: many natural questions about it (like: "what will be the locomotion for a given stroke?", "what is the optimal stroke?", and even simple questions like "what will be the direction the swimmer will swim in a given stroke?") cannot be answered analytically. Even when these questions are answered [3, 6], one gain no intuition about the behavior of the swimmer in different conditions or for different strokes. This is also the case for most of the analyzed swimmer: some of them are too complicated [10, 8], while the simpler swimmers have no optimum [2, 19]. This had motivated us to look for simple swimmers, that can give a better understanding and are a comfortable platform for future work. The simplest swimmer we came up with is, in a sense, a"symmetrization" of the Purcell's three linked

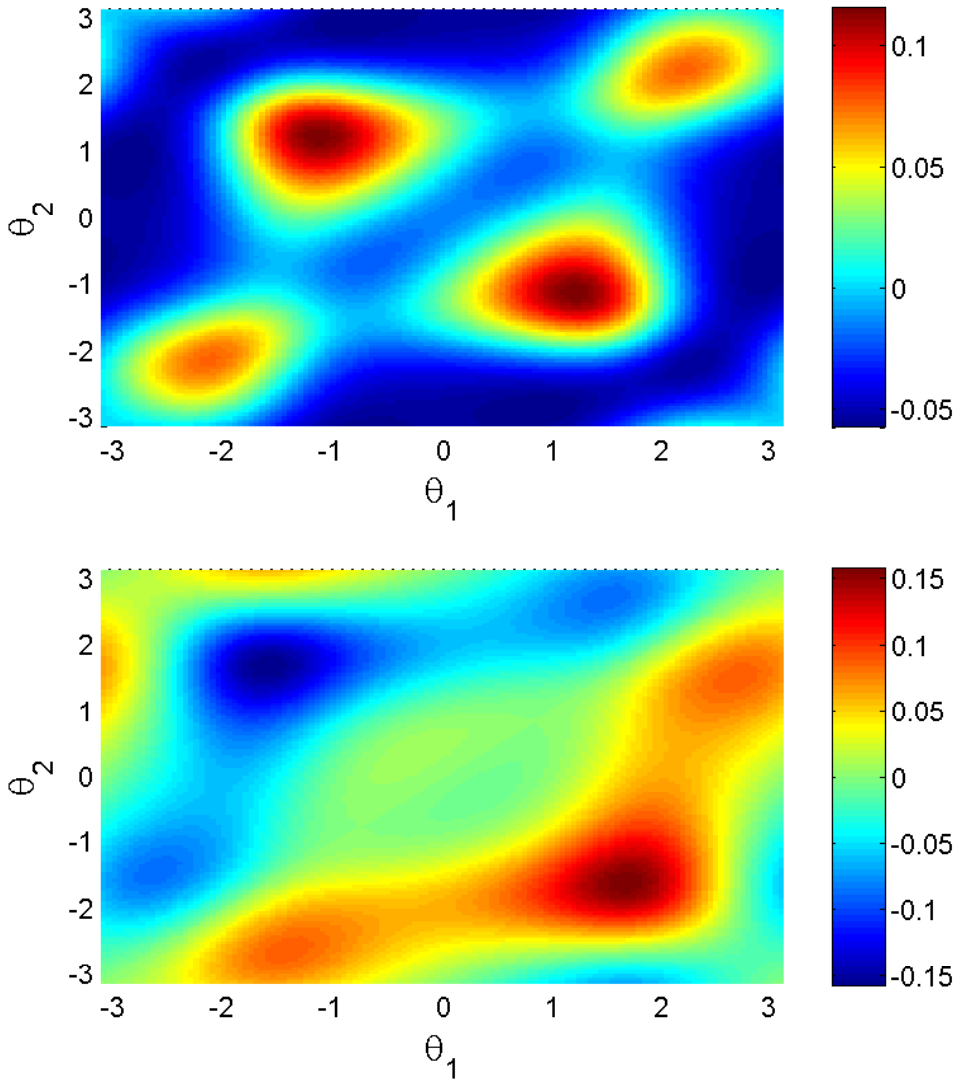

Figure 3: Upper: $\tilde{\mathcal{F}}^y(\theta_1, \theta_2)$, Lower: $\tilde{\mathcal{F}}^x(\theta_1, \theta_2)$ for the Purcell's three linked swimmer (in l_1 units)

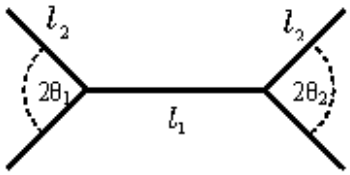

Figure 4: The symmetrized purcell's swimmer

swimmer.

The "symmetric Purcell's swimmer" is made of 5 rods (each one of them with a very small aspect ratio κ): one "body-rod" with length l_2 (which can be zero) and 4 "arms" with the same length l_1, two of them are linked to each end of the body-rod (see fig. 4). The swimmer can control the two opposite angles - the angles between the two arms on each side (θ_1, θ_2), keeping the two arms of each end symmetric around the "body" axes. Being symmetric, this swimmer will not rotate and will swim only in the "body" direction, thus it's motion is in one dimension. Using slender body approximation (Eq. 2.4) and the fact that the total force on the swimmer is zero, one can calculate the velocity of the "body-rod" of the swimmer for every given point in the configuration space (which is a point in the "shape space" (θ_1, θ_2) with the changing in the shape of the swimmer) $(\theta_1, \theta_2, \dot{\theta}_1, \dot{\theta}_2)$:

$$U = \frac{2l_1^2(\sin\theta_1\dot{\theta}_1 - \sin\theta_2\dot{\theta}_2)}{l_2 + 2l_1(2 + \sin^2\theta_1 + \sin^2\theta_2)} \tag{2.9}$$

Since l_2 is only a "dead weight" and reduces the swimmer velocity, we will sometime use the case $l_2 = 0$. In this case the velocity is defined as the velocity of the vertex, and is calculated to be:

$$U = \frac{l_1(\sin\theta_1\dot{\theta}_1 - \sin\theta_2\dot{\theta}_2)}{(2 + \sin^2\theta_1 + \sin^2\theta_2)} \tag{2.10}$$

As in the case of ϕ in the Purcell's swimmer, we can write:

$$\Delta X = \oint_{\gamma} U dt = \oint_{\gamma} A_1(\theta_1, \theta_2) d\theta_1 + A_2(\theta_1, \theta_2) d\theta_2 = \int_{S(\gamma)} F d\theta_1 d\theta_2 \tag{2.11}$$

where $S(\gamma)$ is the oriented surface whose boundary is γ, and $F = \nabla \wedge A$ is called "curvature field" [30] and is given by:

$$F = \frac{-8 l_1 sin\theta_1 sin\theta_2 (cos\theta_1 + cos\theta_2)}{(l_2 + 2 l_1 (2 + sin^2\theta_1 + sin^2\theta_2))^2} \tag{2.12}$$

and in the case $l_2 = 0$ by:

$$F = \frac{-2 l_1 sin\theta_1 sin\theta_2 (cos\theta_1 + cos\theta_2)}{(2 + sin^2\theta_1 + sin^2\theta_2)^2}$$

For any curve γ in the shape space (θ_1, θ_2), the displacement is given by the surface integral Eq. (2.11). As in the case of ϕ of the Purcell's three linked swimmer, $F(\theta_1, \theta_2)$ (plotted in the background of fig. 5) contains all the information about the displacement ΔX of any stroke of this swimmer.

2.4 The most efficient stroke

In the following section we will calculate only the case $l_2 = 0$ for simplicity, since it is clear that this is the optimal swimmer. Looking at F in the background of Fig. (5) one can tell immediately that the stroke for which the displacement is maximal [6], is the triangle in shape space who's vertices are at $(0,0); (0,\pi); (\pi,0)$, and is a "boundary stroke", which cannot be analyzed using slender body approximation [5] to first order.

In order to find the most efficient stroke (which is a more common way to characterize swimmers, and can be extended to many-dimensional shape space swimmers as well), we need to have an expression for the energy dissipation. The energy dissipation of a path γ can be calculated by integrating the power over the time of the stroke. The power is a quadratic expression of $\dot{\theta}_1$ and $\dot{\theta}_2$, and using slender body approximation (Eq. 2.4) again one can calculate that the energy dissipation for a given curve γ is given by

$$E = \int_{\gamma} \frac{1}{2} g_{ab} \dot{\theta}_a \dot{\theta}_b dt \tag{2.13}$$

(summing on a,b), where g_{ab} is given by

$$\begin{aligned} g_{1,1} &= \frac{2\pi\mu}{ln\kappa}\frac{4l_1^3\left(4+2\sin^2\theta_2-\sin^2\theta_1\right)}{3\left(2+\sin^2\theta_1+\sin^2\theta_2\right)} \\ g_{2,2} &= \frac{2\pi\mu}{ln\kappa}\frac{4l_1^3\left(4+2\sin^2\theta_1-\sin^2\theta_2\right)}{3\left(2+\sin^2\theta_1+\sin^2\theta_2\right)} \\ g_{1,2} &= g_{2,1} = \frac{2\pi\mu}{ln\kappa}\frac{4l_1^3\sin\theta_1\sin\theta_2}{3\left(2+\sin^2\theta_1+\sin^2\theta_2\right)} \end{aligned} \tag{2.14}$$

E depends on the time parametrization of γ, but it is known that the minimal energy dissipation is for parametrization for which the power, $P = g_{a,b}\dot{\theta}_a\dot{\theta}_b$, is constant [3]. The expression for the dissipation (Eq. 2.13) has the form of measuring distance, and thus we will call $g_{i,j}$ *a metric* on shape space (the dissipation metric).

Consider the problem of minimizing the energy dissipation of a stroke, subject to the constrain of fixed step size $\Delta X = \oint U dt$. This is a standard problem in variational calculus, and is known [1] to be equivalent to maximizing the efficiency, defined as $\varepsilon = \frac{P_{drag}}{P_{swim}} = \frac{\frac{2\pi}{\ln\kappa}4l_1\left(\int_{S(\gamma)} F(\theta_1,\theta_2)d\theta_1 d\theta_2\right)^2}{\left(\int_{\gamma(\theta_i)}\sqrt{g_{a,b}\frac{d\theta_a}{d\theta_i}\frac{d\theta_b}{d\theta_i}}d\theta_i\right)^2}$ [20]. Note that since one may set $\tau = 1$ without loss, fixing the average speed is equivalent to fixing the step size $X(\gamma)$. The minimizer, $\gamma(t)$, must then either follow the boundary or solve the Euler-Lagrange equation of the functional

$$S_\lambda(\gamma) = \int_0^\tau \frac{1}{2}g_{a,b}\dot{\theta}_a\dot{\theta}_b dt + \lambda\int_0^\tau \frac{l_1(\sin\theta_1\dot{\theta}_1 - \sin\theta_2\dot{\theta}_2)}{(2+\sin^2\theta_1+\sin^2\theta_2)}dt \tag{2.15}$$

where λ is a Lagrange multiplier, and there is a summation convention on a, b. For each initial conditions, one can find the optimal stroke by solving the Euler-Lagrange equations of the action in Eq. (2.15). The optimal stroke is plotted in figure (5)(computed numerically). The efficiency for this stroke is 0.0079, which is about the same as the efficiency of the Purcell's swimmer for rectangular strokes [3], but less then the efficiency for general strokes [6].

2.5 Swimming in different viscosities

Till now, we assumed that the swimmer can control it's shape directly. This may not always the case: some artificial swimmers (and probably some biological swimmers as well) cannot control their shape directly, but can control the changes in their shape: they are using constant power in fixed time parametrization, so changing the viscosity changes the stroke. For example, consider the Purcell's three linked swimmer, made of

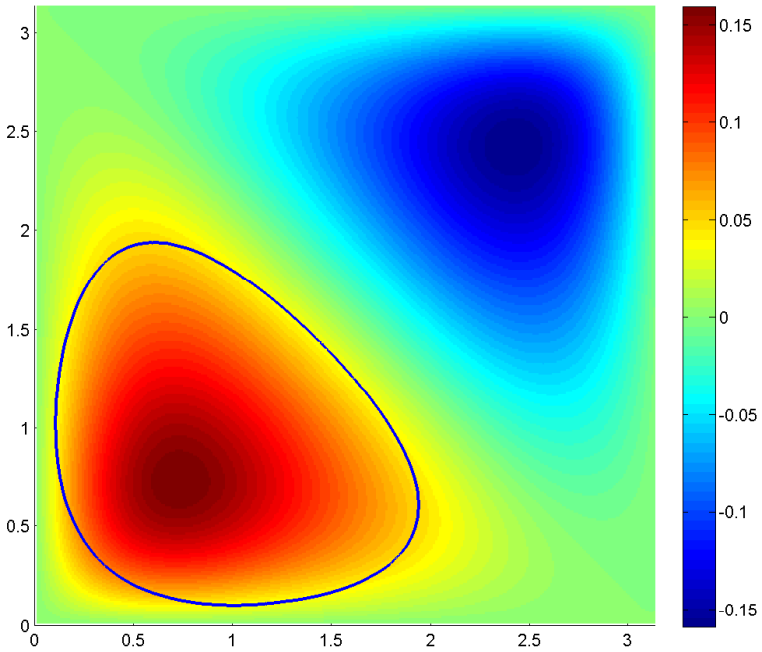

Figure 5: The optimal stroke for the symmetric purcell swimmer, plotted on $F(\theta_1, \theta_2)$ for this swimmer

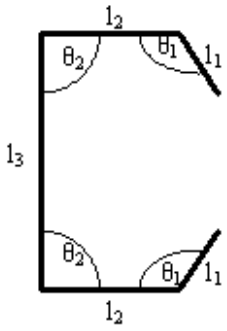

Figure 6: 5-Links, A swimmer which changes its moving direction when putted in more viscous fluid

three rods with two engines (which changes the angles between the rods), and performing rectangular strokes (that is - the engines are working one-by-one). Now, assume that each engine works with constant power for constant time. In this case - each engine can change the shape of the swimmer by certain distance in shape space according to the dissipation metric. Since the metric does depend on the viscosity, the swimmer will do different strokes in different fluids: the more viscose the fluid, the smaller the stroke will be. While in some cases making the stroke smaller will lead to smaller displacement, in cases the curvature changes it sign (as in the case of Purcell's swimmer) making smaller strokes may lead to larger displacement.

In order to be more concrete, we will introduce another example of a symmetric swimmer: this swimmer (which we call "5-Links") is again made of five rods, this time all in a line (Fig. 6). The swimmer is symmetric around the central vertical of the middle link, and thus can control only two angels: θ_1 is the angle between the firs rod and second one (the forth and fifth rods), and θ_2 is the angle between the second and third rods (third and forth rods). We will note the length of the first (fifth) rod as l_1 (this will be our length units), the second (forth) rod as $l_2 = 10l_1$ and the middle rod as $l_3 = 30l_1$. In order for the arms not to collide, we will limit the shape space (θ_1, θ_2) to be $[0.2, 2\pi - 0.2] \times [0.2, pi - 0.2]$.

The analog for Eq. (2.12) (which is, again, not a simple expression and will not be given here) is plotted in Fig. (7). As one can see from the figure, a stroke which is a rectangle

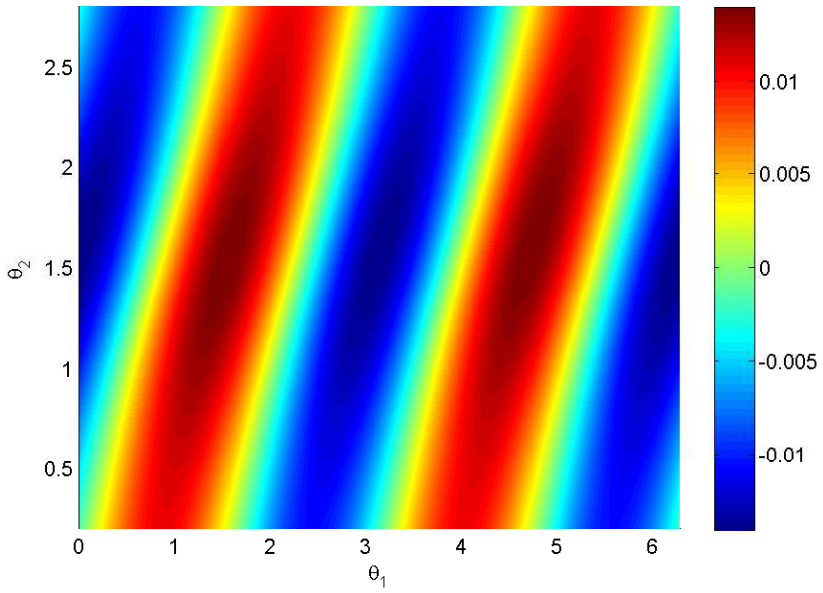

Figure 7: $F(\theta_1, \theta_2)$ for the 5-Links swimmer

in (θ_1, θ_2) around $(\pi, \frac{\pi}{2})$ will lead to locomotion in different directions - depending on the amplitude of the stroke. It is clear in this case that there is some regime in which making smaller strokes will lead to larger displacement.

The power has the following properties:

- It is quadratic in $\dot{\theta}_{1,2}$, and can again be written as $P = g_{a,b}\dot{\theta}_a\dot{\theta}_b$. $g_{a,b}$ can be thought of as a metric on shape space.
- It is symmetric around $\theta_1 = \pi$ and $\theta_2 = \frac{\pi}{2}$. Thus a rectangular power stroke, that is - a stroke in which θ_1 and θ_2 are changed one by one, and the power for each change is constant for a constant time, is also a rectangle in shape space (provided it starts from a point on the curve in shape space).
- The power is linear in μ, so changing the viscosity of the fluid will change the amplitude of the stroke.

If we will fix the power of the engines changing $\theta_{1,2}$ so that in some fluid with viscosity μ_0 the stroke is symmetric around $(\pi, \frac{\pi}{2})$ and will cover equal amount of negative and positive $F(\theta_1, \theta_2)$, putting the swimmer in more viscous fluid ($\mu > \mu_0$) will lead to a larger displacement, at least for some values of μ.

3 Swimming, Pumping and Gliding at low Reynolds number

3.1 Introduction

Low Reynolds numbers hydrodynamics governs the locomotion of tiny natural swimmers such as micro-organisms and tiny artificial swimmers, such as microbots. It also governs micro-pumps [26], tethered swimmers [7, 27] and gliding under the action of external forces. Our purpose here is to discuss some interesting consequences of simple, yet general and exact relations that relate pumping, swimming and gliding at low Reynolds numbers. The equations are not new, and appear for example in [31, 28], where they serve to analyze swimming at low Reynolds numbers. The interpretation of these equations as a relation between three apparently different objects: Swimmers, pumps and gliders, gives them a new and different flavor and suggests new applications which we explore below.

Our first tool is Eq. (3.16) which relates the velocity of a free swimmer to the (torque and) force needed to anchor it to a fixed location. This equation appears in the analysis of swimmers [31, 28]. It can be applied to experiments on tethered swimmers [4, 16, 32] where it can be used to infer the velocity of a free swimmers from measurements of the force on tethered one (and vice versa) and when both are measured, to an estimate of the gliding resistance matrix M of Eq. (3.18).

Our second tool is Eq. (3.22) which says that the power needed to operate a pump — a tethered swimmer — is the sum of the power invested by the corresponding free swimmer, and the power needed to tow it. (The result holds for arbitrary container of any shape or size). It is useful in studying and comparing the efficiencies of swimmers and pumps. In particular, it says that a tethered swimmer spends *more power* than a free swimmer. As we shall see it also implies that it is impossible to pump with arbitrary high efficiency.

Physically, both relations may be viewed as an expression of the elementary observation that swimmers and pumps are the flip sides of the same object: A tethered swimmer is a pump [7] and an unbolted pump swims. This observation plays limited role in high Reynolds numbers, because it does not lead to any useful equations for the non-linear Navier Stokes equations. For microscopic objects, where the equations reduce to the linear Stokes equations, the observation translates to linear relations.

Formally, a pump is a swimmer with a distinguished point — the point of anchoring. The pump may have different properties depending on the point of anchoring, (we shall

see an example where it pumps in different directions depending on the anchoring point). We shall solve a problem, posed by E. Yariv [31], of how to find the optimal anchoring point for a certain class of swimmers, which we call "linear swimmers". The class includes the Purcell swimmer [23], the "three linked spheres" [10] and pushmepullyou [2].

There are various notions of optimality that one needs to consider in the study of swimmers and pumps. For swimmers, one notion of optimality is to maximize the distance covered in one stroke. A different notion is to minimize the dissipation in covering a given distance at a given speed. Similarly, for a pump one may want to maximize the momentum transfer to the fluid in one stroke, or, alternatively, to minimize the dissipation for given total momentum transfer and rate. How are optimal swimmers related to optimal pumps? We study this question for helices and show that optimal swimmers and pumps have different geometry: There are four optimal pitch angles depending on what one optimizes and whether the helix is viewed as a swimmer or a pump.

3.2 Anchoring as a choice of gauge

Let us start by briefly discussing the gauge issues that arise when considering swimming [30], pumping and gliding.

Fixing a gauge is already an issue for a glider. A glider is a rigid body undergoing an Euclidean motion under the action of an external force. There is no canonical way to decompose a general Euclidean motion into a translation and a rotation [18]. Such a decomposition requires choosing a fiducial reference point in the body to fix the translation. In the theory of rigid body a natural choice is the center of mass. This is, however, *not* a natural choice at low Reynolds number. This is because this is the limit when inertia plays no role and the glider may be viewed as massless. Since the choice becomes arbitrary, it may be viewed as a choice of gauge.

In the case of a swimmer one needs to fix a point arbitrarily and in addition, to fix a fiducial frame. This is because a swimmer is a deformable body and such a frame is required to fix the rotation [30]. This is, again, a choice of gauge.

A pump is an anchored swimmer with a distinguished point and a distinguished frame which are determined by the way the pump is anchored. When we write equations that involve swimmers, pumps and gliders, we pick the fiducial point and frame determined by the the way the pump is anchored.

3.3 Triality of swimmer pumps and gliders

Capital bold letters will be used for 6 dimensional vectors, non-bold Capital letters for 3 dimensional vectors and bold non-Capital letters for 3 dimensional vector fields.

We shall first recall the derivation of the linear relation between the 6 dimensional force-torque vector, $\vec{\mathbf{F}}_p = (\vec{F}_p, \vec{N}_p)$ which keeps a *pump* anchored with fixed position and orientation, and the 6 dimensional velocity–angular-velocity vector, $\vec{\mathbf{V}}_s = (\vec{V}_s, \vec{\omega}_s)$ associated with the corresponding *autonomous swimmer*:

$$\vec{\mathbf{F}}_p = -M\,\vec{\mathbf{V}}_s, \tag{3.16}$$

This holds for all times ($\vec{\mathbf{F}}_p, M$ and $\vec{\mathbf{V}}_s$ are time dependent quantities). M is a 6×6 matrix of linear-transport coefficients of the corresponding *glider*:

$$\vec{\mathbf{F}}_g = M\,\vec{\mathbf{V}}_g \tag{3.17}$$

namely, the corresponding rigid body, moving at (generalized) velocity $\vec{\mathbf{V}}_g$ under the action of the (generalized) force $\vec{\mathbf{F}}_g$. Note the change in sign. The matrix M depends on the geometry of the body. It is a positive matrix of the form [12]:

$$M = \begin{pmatrix} K & C \\ C^t & \Omega \end{pmatrix} \tag{3.18}$$

where K, C, and Ω are 3×3 real matrices. Note that Eq. (3.17) fails in two dimensions [17].

Eq. (3.16) follows from the linearity of the Stokes equations and the no-slip boundary conditions. Let $\partial\Sigma$ denote the surface of the device. Any vector field on $\partial\Sigma$ can be decomposed into a deformation and a rigid body motion as follows: Any rigid motion is of the form $\vec{\mathbf{v}}_g = \vec{V} + \vec{\omega} \times \vec{\mathbf{x}}$. Pick $\vec{V}$ to be the velocity of a fiducial point and $\vec{\omega}$ the rotation of the fiducial frame. The deformation field is then, by definition, what remains when the rigid motion is subtracted from the given field $\vec{\mathbf{v}}$.

Now, decompose $\vec{\mathbf{v}}_s$ the velocity field on the surface of a swimmer, to a deformation and rigid-motion as above. The deformation field can be identified with the velocity field at the surface of the corresponding pump $\vec{\mathbf{v}}_p$ since the pump is anchored with the fiducial frame that neither moves nor rotates. The remaining rigid motion $\vec{\mathbf{v}}_g$ is then naturally identified with the velocity field on the surface of the glider. The three vector fields are then related by

$$\vec{\mathbf{v}}_s = \vec{\mathbf{v}}_p + \vec{\mathbf{v}}_g, \quad \vec{\mathbf{v}}_g = \vec{V}_s + \vec{\omega}_s \times \vec{\mathbf{x}} \tag{3.19}$$

where $\vec{V}_s$ is (by definition) the swimming velocity and $\vec{\omega}_s$ the velocity of rotation.

Each of the three velocity fields on $\partial\Sigma$, (plus the no-slip zero boundary conditions on the surface of the container, if there is one), uniquely determine the corresponding velocity field and pressure $(\vec{\mathbf{v}}, p)$ throughout the fluid. The stress tensor, π_{ij}, depends linearly on $(\vec{\mathbf{v}}, p)$ [17] .

By the linearity of the Stokes and incompressibility equations Eq. (1.2), it is clear that $\vec{\mathbf{v}}_s = \vec{\mathbf{v}}_g + \vec{\mathbf{v}}_p$ and $p_s = p_g + p_p$ and then also $\pi_s = \pi_p + \pi_g$. Since $F_i = \int_{\partial\Sigma} \pi_{ij} dS_j$ is the drag force acting on the device we get that the three force vectors are also linearly related: $\vec{F}_s = \vec{F}_p + \vec{F}_g$, and similarly for the torques. This is summarized by the force-torque identity $\vec{\mathbf{F}}_s = \vec{\mathbf{F}}_p + \vec{\mathbf{F}}_g$. Since the force and torque on an autonomous Stokes swimmer vanish, Eq. (3.16) follows from Eq. (3.17).

Eq. (3.16) has the following consequences:

- Micro-Pumping and Micro-Stirring is geometric: The momentum and angular momentum transfer in a cycle of a pump, $\int \vec{\mathbf{F}}_p dt$, is independent of its (time) parametrization. In particular, it is independent of how fast the pump runs. This is because swimming is geometric [23, 30] and the matrix M is a function of the pumping cycle, but not of its parametrization.

- Scallop theorem for pumps: One can not swim at low Reynolds numbers with self-retracing strokes. This is known as the "Scallop theorem" [23]. An analog for pumps states that there is neither momentum nor angular momentum transfer in a pumping cycle that is self-retracing. This can be seen from the fact that $\vec{\mathbf{V}}_s\, dt$ is balanced by $-\vec{\mathbf{V}}_s\, dt$ when the path is retraced, and this remains true for $M\vec{\mathbf{V}}_s\, dt$.

We shall now derive an equation, originally due to [28], which relates the power expenditure of swimmers, pumps and gliders. It follows from Lorentz reciprocity for Stokes flows, discussed at section 1.3, that says that if (v_j, π_{jk}) and (v'_j, π'_{jk}) are the velocity and stress fields for two solutions of the Stokes equations in the domain Σ then [12]:

$$\int_{\partial\Sigma} v'_i\, \pi_{ij}\, dS_j = \int_{\partial\Sigma} v_i\, \pi'_{ij}\, dS_j \tag{3.20}$$

For the problem at hand, we may take $\partial\Sigma$ to be the surface of our device (since the velocity fields vanish on the rest of the boundary associated with the container). The area element $\vec{dS}$ is chosen normal to the surface and pointing into the fluid. Now apply the Lorentz reciprocity to a pump and a swimmer velocity fields and use Eq. (3.19) on both sides. This gives

$$-P_s + \vec{\mathbf{V}}_s \cdot \vec{\mathbf{F}}_s = -P_p - \vec{\mathbf{V}}_s \cdot \vec{\mathbf{F}}_p \tag{3.21}$$

where P_s is the power invested by the swimmer and P_p the power invested by the pump. Since the force and torque on the swimmer vanish, $\vec{\mathbf{F}}_s = 0$, we get, using Eq. (3.16) a linear relation between the powers:

$$P_p - P_s = -\vec{\mathbf{V}}_s \cdot \vec{\mathbf{F}}_p = \vec{\mathbf{V}}_s \cdot M\vec{\mathbf{V}}_s = P_g \geq 0 \tag{3.22}$$

P_g is the power needed to tow the glider. Since both swimming and towing require positive power, at any moment pumping is more costly than swimming or dragging[1].

The linearity of Eq. (3.22) is a noteworthy, and somewhat unexpected. Eq. (3.19) says that the corresponding velocity fields are linearly related. Since power at low Reynolds number is quadratic in the velocity a linear relation between the powers is not what one may naively expect.

The most interesting consequence of this relation which, at least for us, was somewhat of a surprise, is that a pumps needs more power than a swimmer and so the power consumed by a tethered swimmer is actually an upper bound on the power consumed by it when freed.

One of the remarkable facts about low Reynolds number swimming is that even though the dynamics is governed by dissipation it is still possible to swim with arbitrarily high efficiency [2, 19]. For this to happen, the swimming velocity should be non-zero, but the energy dissipation of the swimmer, P_s, should be zero, thus $P_p = P_g \geq 0$. The same cannot happened for pumps: for a pump to be with arbitrarily high efficiency, it must have non-zero momentum transfer to the fluid and zero power. Since M of Eq. (3.18) is a strictly positive matrix P_g is quadratic in the force and can not vanish if the pump transfers momentum to the fluid.

3.4 Linear swimmers and optimal anchoring

E. Yariv [31] posed the following problem: Find the anchoring point which optimizes the momentum transfer to the fluid. The general case is complicated. A class of swimmer for which this question can be answered relatively easily is the class of "linear swimmers" — swimmers made of segments, so that the velocity of different points on the same segment depend linearly on the distance between the points. This class contains the three linked spheres [10], the pushmepullyou [2], Purcell's three linked swimmer [3, 6], the 'N-Linked' swimmer [8], but not, for example, the treadmiller [19].

[1] In the case that the pump is allowed to rotate M is replaced by K and $\vec{\mathbf{V}}_s$ by $\vec{V}_s$.

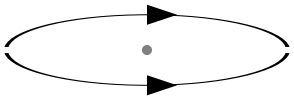

Figure 8: A treadmiller transports its skin from head to back. The treadmiller in the figure swims to the left while the motion of its skin guarantees that,in the limit of large aspect ratio, the ambient fluid is left almost undisturbed. If it is anchored at the gray point then it transfers momentum to the fluid (to the right). The power of towing a frozen treadmiller and of pumping almost coincide reflecting the fact that a treadmiller swims with little dissipation.

Shifting the anchoring point by $\vec{r}$, the resistance matrixes K, C and Ω of Eq. 3.18 will be changed to $K_r = K$, $C_r = C - KR$ and $\Omega_r = \Omega - RKR + CR - RC^t$ [12], where R is the antisymmetric matrix associated with the vector $\vec{r}$. The change in $\vec{V}_s$ is linear in $\vec{r}$, and $\vec{\omega}_s$ is unchanged [18]. Using Eq. (3.16), the change in the force $\vec{F}_p$ (and hence in the linear-momentum transfer to the fluid) is linear with $\vec{r}$, and the optimal point which maximized the force must be at one of the edges of the segments.

(The change in the torque $\vec{T}_p$ (and hence in the angular-momentum transfer to the fluid) is quadratic in $\vec{r}$, so the maximum can be either at the edges, or at the point in which the differential of the angular momentum with respect to the anchoring point is zero (in cases where there is such a point). In either case, one has to check only a few points.)

A case in point is the "three linked spheres" [10]. There are three candidates for the optimal anchoring point: The three spheres. The two outer spheres are related by symmetry so the two interesting cases are either anchoring on an outer sphere or in the middle sphere. Detailed calculations show (appendix A) that the maximum momentum transfer will be when the anchoring point is on one of the outer spheres. When the swimmer is anchored on the middle sphere, the momentum transfer turns out to be *in the opposite direction*. Calculation for the efficiency shows that the optimal point in this case is also at the outer spheres.

3.5 Helices as swimmers and pumps

Eq. (3.16) and Eq. (3.22) have an analogs for non-autonomous rigid swimmers such as a helix rotating by the action of an external torque [25]. This is a case that is very easy to treat separately. From Eq. (3.17) applied to the helix twice, once as swimmer and once as a pump we get the analog of Eq. (3.16):

$$\vec{F}_p = C\vec{\omega} = -K\vec{V}_s \tag{3.23}$$

The analog of Eq. (3.22) follows immediately from the definition of the power $P = -\vec{\mathbf{F}} \cdot \vec{\mathbf{V}}$ and Eq. (3.17) again:

$$P_p - P_s = \vec{\mathbf{F}}_p \cdot \vec{\mathbf{V}}_p - \vec{\mathbf{F}}_s \cdot \vec{\mathbf{V}}_s = -\vec{V}_s \cdot \vec{F}_p = P_g \tag{3.24}$$

It follows from this that the difference in power between a swimmer and a pump is minimized, for given swimming velocity, if the swimming direction coincides with the smallest eigenvalue of K which is the direction of optimal gliding.

The distinction between optimal pumps and optimal swimmers [24] can be nicely illustrated by the considering the example of a rotating helix, or a screw. This motion has been studied carefully in [20, 13] whose analysis goes beyond what we need here. For a thin helix the slender-body theory [5], discussed earlier in section 2.2, can be used. Consider a helix of radius r, pitch angle θ and total length ℓ. The helix is described by the parameterized curve

$$(r\cos\phi, r\sin\phi, t\sin\theta), \quad \phi = \frac{t}{r}\cos\theta, \quad t \in [0, \ell] \tag{3.25}$$

Suppose the helix is being rotated at frequency ω about its axis. Substituting the velocity field of a rotating helix, with an unknown swimming velocity in the z-direction, into Eq. (2.4), and setting the total force in the z-direction to zero, fixes the swimming velocity. Dotting the force with the velocity and integrating gives the power. This slightly tedious calculation gives for the swimming velocity (along the axis) and the power of swimming:

$$\frac{V_s}{\omega r} = \frac{\sin 2\theta}{3 + \cos 2\theta}, \quad \frac{P_s}{k\ell\omega^2 r^2} = \frac{4}{3 + \cos 2\theta} \tag{3.26}$$

Similarly, for the pumping force and power one finds

$$\frac{F_p}{k\ell\omega r} = \sin\theta\cos\theta, \quad \frac{P_p}{k\ell\omega^2 r^2} = 1 + \sin^2\theta \tag{3.27}$$

Eq. (3.26) and (3.27) have the following consequences for optimizing pumps and swimmers:

- Given ωr, a swimmer velocity V_s is maximized at pitch angle $\theta = 54.74°$.
- Given ωr, the pumping force F_p is maximized at $\theta = 45°$.

Consider now optimizing *both* the pitch angle θ and rotation frequency ω so that the swimming velocity is maximized for a given power. Namely

$$\max_{\theta,\omega}\{V_s \mid P_s = const\} \tag{3.28}$$

and similarly for pumping, except that F_p replaces V_s and P_p replaces P_s. A simple calculation shows that this is equivalent to optimizing V_s^2/P_s and F_p^2/P_p with respect to θ. (These ratios are independent of ω and so invariant under scaling time). One then finds:

- The efficiency of swimming, V_s^2/P_s, is optimized at $\theta = 49.9°$. The efficiency is proportional to $(k\ell)^{-1}$ which favors small swimmers in less viscous media, as one physically expects.
- The efficiency of pumping, F_p^2/P_p, is optimized at $\theta = 42.9°$. The efficiency is proportional to $(k\ell)$ which favors big pumps at more viscous media. Micro-pumps are perforce inefficient.

There is a somewhat unrelated, yet insightful fact that one learns from the above computation regarding the difference between motion in a very viscous fluid and motion in a solid. The naive intuition that the two are similar at very high viscosity would imply that a helix moves like a cork-screw and so would move one pitch in one turn. This is actually never the case, no matter how large μ is. In fact, the ratio of velocities of a helix to a cork-screw is independent of μ and by Eq. (3.26)

$$\frac{V_s}{\omega r \sin\theta} = \frac{\cos\theta}{1+\cos^2\theta} \leq \frac{1}{2} \tag{3.29}$$

A helix needs at least two turns to advance the distance of its threads.

3.6 Pumps that do not swim

We have noted that the "three linked spheres" can pump either to the right or to the left depending on whether it is anchored on the center sphere or on an external sphere. There is, therefore, an intermediate point where it will not pump.

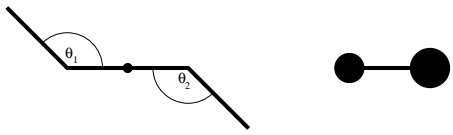

Figure 9: A Purcell three linked swimmer, left, controls the two angles θ_1 and θ_2. When bolted it effectively splits into two independent wind-shield wipers each of which is self retracing. It will, therefore, not pump. Pushmepullyou, right, controls the distance between the two spheres and the ratio of their volumes. It can have arbitrarily large swimming efficiency.

There are also pumps that will not swim: Evidently, if the swimming stroke is right-left and up-down symmetric, the swimmer will not move by symmetry. It can, however, be bolted in a way that breaks the symmetry to give an effective pump. For example - consider a right-left symmetric pushmepullyou [2], where the two spheres inflate and deflate in phase. By symmetry, it will not swim, however, anchoring in any point except the middle point will lead to net momentum transfer.

4 Summary

Swimming at low Reynolds number is geometric [30]. E. M. Purcell, who was the first to point this out[23], invented a very simple swimmer, made of three link (see Fig. 1), to emphasize the geometric nature of swimming at low Reynolds number. In this work we explore this swimmer using geometric tools. Although this point of view does not lead to any analytical expression which helps us understanding this swimmer better, it does let us to visualize how the swimmer will behave in the small strokes regime, and how approximately it will behave in large strokes as well (see Fig. (2) and Fig. (3)). This visualization tools can help us in searching for the optimal strokes [22, 6], and can explain some "wired" behavior of the swimmer, like the fact that it swims in different directions when the amplitude of the stroke changes [3]. Since this swimmer turns out to be very complicated to analyzed, we introduce a much simpler swimmer, made of 5 rods, which is in some sense a "symmetrization" of the original Purcell's three linked swimmer. Being symmetric, this swimmer cannot rotate, and calculating analytically his velocity, locomotion per stroke and energy dissipation, is very easy. This let us find the optimal stroke for this swimmer.

In many cases, a swimmer cannot control it's shape directly, but only the power he used to change it's shape. In such cases, the swimming will be medium dependent: the energy dissipation of the swimmer form a metric on shape space. This metric depends on the viscosity of the fluid, so the swimmer will do different strokes in different fluids: the swimmer is performing a stroke with a fixed length in the dissipation metric. This definition of a stroke can lead to a swimming with larger displacement in more viscose fluid, which is the case in a new swimmer (the "5-Links") we introduce. The motivation for this definition is a micro-organism, Spiroplasma [9], who is known to swim better in more viscose fluids. The actual reason for the Spiroplasma to swim better in more viscose fluid is unknown, and the "5-Links" swimmer shows one model this might happened.

After studying swimmers, we turn to studying the relations between a swimmer and the pump one would get by anchoring the swimmer. The motivation for this research is the experimental simplicity of measuring anchored swimmer instead of free ones, and the need for pumps for micro-fluid devices. In order to relate swimmers to pump we use the linearity of the Stokes equation, and the Lorenz reciprocity. The relations we get for the force–velocity and the powers are very simple, and relate pumps to swimmers through a glider - which is a frozen swimmer dragged by an external force. They say that a pump will always use more power then the swimmer, and shed light on why it is possible to swim with arbitrarily low energy cost but it is impossible to pump with arbitrarily low

energy cost.

We give some examples to the use of the relations between pump and swimmer: we answer the question of "Where to anchor a given swimmer to get the pump with largest momentum transfer" for a class of swimmer we call "linear swimmers" which include many of the swimmers like the Purcell's three linked swimmer, the three linked spheres, the Pushmepullyou and the N-linked swimmer. We calculate the pitch angle for a helix in the case of pump and a swimmer, optimizing the velocity, force, and efficiency. We get 4 different pitches for the 4 cases. We end up by showing that there are cases of a swimmer that will not pump and a pump that will not swim.

A The three linked swimmer as a pump

The three linked spheres [10], is a simple swimmer made of three spheres with radiuses a in a line, located at $x_1, x_2 = x_1 + q_1, x_3 = x_2 + q_2$, which can control the two distances q_1 and q_2. This swimmer can be analyzed using the Oseen tensor (which is a good approximation for the case $q_i >> R; \quad i = 1, 2$): the force on the i sphere is given by [12]:

$$F_i = \sum_{j=1}^{3} H_{ij} V_j \quad with \quad \begin{cases} H_{ii} = -6\pi\mu a \\ H_{ij} = -6\pi\mu a \frac{3R}{X_{ij}} \\ X_{ij} = |x_i - x_j| \end{cases} \tag{A.30}$$

The total momentum transferred to the fluid in one stroke can be calculated by integrating $\sum_{i=1}^{3} F_i$ over a complete stroke cycle. The total momentum transfer is invariant under changes in the time parametrization: $\Delta Momentum = \int \sum_{i=1}^{3} F_i dt = \int \sum_{i,j=1}^{3} H_{ij} dx_j$. Here we will analyze this swimmer for the simple case of rectangular strokes: we start with $q_1 = q_2 = q$, and in the strokes we change q_1 to be $q + \Delta q$, then q_2 to be $q + \Delta q$, then changing q_1 back to q and then changing q_2 to q. When anchoring the swimmer in one of the outer spheres (the left one, in this example), the total momentum transfer for the stroke is given (calculating the integral over the stroke using Mathematica) by:

$$-\frac{18\pi a^2 \Delta q^2}{q(q + \Delta q)}$$

which is a negative expression, corresponding the fact that the momentum transfer is to the left. When anchoring the swimmer at the middle sphere, the total momentum transfer for the stroke is given (calculating the integral over the stroke using Mathematica) by :

$$-18\pi a^2 \ln\left(\frac{4q(q + \Delta q)}{4q(q + \Delta q) + \Delta q^2}\right)$$

Since the denominator in the ln is grater than the numerator, the sign of the ln is negative, and this expression is positive: the total momentum transfer in this case is to the right!

References

[1] J. E. Avron, O. Gat, and O. Kenneth. Optimal swimming at low reynolds numbers. *Physical Review Letters*, 93(18):186001, 2004.

[2] J. E. Avron, O. Kenneth, and D. H. Oaknin. Pushmepullyou: an efficient micro-swimmer. *New Journal of Physics*, 7:234–242, 2005.

[3] L. E. Becker, S. A. Koehler, and H. A. Stone. On self-propulsion of micromachines at low reynolds number: Purcell's three-link swimmer. *J. of Fluid Mechnics*, 490:15–35, 2003.

[4] S. Chattopadhyay, R. Moldovan, C. Yeung, and X. L. Wu. Swimming efficiency of bacterium escherichia coli. *PNAS*, 103(13):13712–13717, September 2006.

[5] R.G. Cox. The motion of long slender bodies in a viscous fluid part 1. general theory. *J. Fluid Mechanics*, 44(4):791–810, December 1970.

[6] A. E. Hosoi D. Tam. Optimal stroke patterns for purcell's three-linked swimmer. *Physical Review Letters*, 98:4, February 2007.

[7] Nicholas Darnton, Linda Turner, Kenneth Breuer, and Howard C. Berg. Moving fluid with bacterial carpets. *Biophysical Journal*, 86(4):1863, 2004.

[8] Gerusa Alexsandra de Araujo and Jair Koiller. Self-propulsion of n-hinged 'animals' at low reynolds number. *QUALITATIVE THEORY OF DYNAMICAL SYSTEMS*, 4(58):139–167, 2004.

[9] Trachtenberg S. Gilad R., Porat A. Motility modes of spiroplasma melliferum bc3: ahelical, well-less bacterium deriven by linear motor. *Molecular Micribiology*, 47(3):657–669, February 2003.

[10] R. Golestanian and A. Najafi. Simple swimmer at low reynolds number: Three linked spheres. *Phys. Rev. E*, 69:062901–062905, 2004.

[11] R. R. Netz H. Wada. Model for self-propulsive helical filaments: Kink-pair propagation. *Phys. Rev. Lett*, 99:108102–1:4, September 2007.

[12] J. Happel and H. Brenner. *Low Reynolds number hydrodynamics*. Kluwer, second edition, 1963.

[13] J. J. L. Higdon. The hydrodynamics of flagellar propulsion: helical waves. *J. Fluid Mechanics*, 94(02):331–351, September 1979.

[14] M. Draper R. T. Kelly A. T. Woolley J. W. Munyan, H.V. Fuentes. Electrically actuated, pressure-driven microfluidic pumps. *Lab on a Chip Comm.*, 3:217–220, 2003.

[15] H. C. Berg R. Montgomery K. M. Ehlers, A. D. T. Samuel. Do cyanobacteria swim using traveling surface waves? *Proc. Natl. Acad. Sci.*, 93:8340–8342, August 1996.

[16] G. Kosa, M. Shoham, and M. Zaaroor. Propulsion of a swimming micro medical robot. *Robotics and Automation*, 2005.

[17] L. D. Landau and I. M. Lifshitz. *Fluid Mechanics*. Pergamon, 1959.

[18] L. D. Landau and I. M. Lifshitz. *Mechanics*. Butterworth and Heinemann, 1981.

[19] A.M. Leshansky, O. Kenneth, O. Gat, and J.E. Avron. A frictionless microswimmer. *New J. Phys.*, 2007.

[20] J. Lighthill. *Mathematical Biofluid-dynamics*. Society of Industrial and Applied Mathematics, 1975.

[21] J. Baudry M. Fermigier J. Bibette H. A. Stone M. Roper, R. Dreyfus. On the dynamics of magnetically driven elastic filaments. *J. Fluid Mechanics*, 554:167–190, 2006.

[22] J. E. Avron O. Raz. A comment on "optimal stroke patterns for purcell's three-linked swimmer". *Phys. Rev. Lett*, in preprint.

[23] E. M. Purcell. Life at low reynolds number. *American Journal of Physics*, 45(1):3–11, January 1977.

[24] M. E. Purcell. The efficiency of propulsion by a rotating flagellum. *PNAS*, 94:1130711311, October 1997.

[25] Dreyfus R., Baudry J., Roper M. L., Fermigier M., Stone H. A., and Bibette J. Microscopic artificial swimmer. *Nature*, 436:862–865, 2005.

[26] 2000 R. F. Day, H. A. Stone :. Lubrication analysis and boundary integral simulations of a viscous micropump. J. of Fluid Mechanics, 416:197–216, 2000.

[27] K. Levit-Gurevich S. Gueron. Energetic considerations of ciliary beating and the advantage of metachronal coordination. *PNAS*, 96:12240–12245, October 1999.

[28] Samuel A. D. T Stone H. A. Propulsion of microorganisms by surface distortions. *Phys. Rev. Lett.*, 77(19):4102–4104, November 1996.

[29] G. I. Taylor. Analysis of the swimming of microscopic animals. *Proc. R. Soc. Lond. A*, 209:447461, 1951.

[30] F. Wilczek and A. Shapere. Geometry of self-propulsion at low reynolds number. *J. of Fluid Mechanics*, 198:557–585, 1989.

[31] E. Yariv. Self-propulsion in a viscous fluid: arbitrary surface deformations. *J. Fluid Mechanics*, 550:139148, 2006.

[32] Tony S. Yu, Eric Lauga, and A. E. Hosoi. Experimental investigations of elastic tail propulsion at low reynolds number. *arXiv:cond-mat/0606527*, 2006.